

NONCONTACT PYROELECTRIC TEMPERATURE METERS WITH SOLID-STATE MODULATOR

L.V. LEVASH, A.I. LIPTUGA¹, V.S. LYSENKO,
YU.G. PTUSHYNSKY, V.B. SAMOYLOV

UDC 536. 5.537.227

©2009

Institute of Physics, Nat. Acad. of Sci. of Ukraine

(46, Nauky Ave., Kyiv 03680, Ukraine),

¹V.E. Lashkarev Institute of Semiconductor Physics, Nat. Acad. of Sci. of Ukraine

(41, Nauky Ave., Kyiv 03680, Ukraine)

The properties of an injection semiconductor modulator of infrared (IR) radiation have been studied. The modulator is found to be a source of its own thermal radiation, which essentially complicates the procedure of weak radiation fluxes measurement. The properties of this radiation have also been studied. We have developed an original modulation block which allows one to compensate the influence of the modulator radiation on the accuracy of low intensity fluxes measurements. The design of a pyroelectric noncontact meter of local temperature with electronic radiation modulation, as well as its operation mechanism and basic parameters, are described.

The noncontact monitoring of the temperature-dependent parameters of technological processes, the temperature regimes of mobile elements in electrical and mechanical facilities, as well as the state of objects that are located at hard-to-reach places, is a challenging problem. Below, we report the results of our development of a noncontact temperature meter constructed on the basis of pyroelectric detectors of IR radiation [1]. The majority of devices used for IR measurements contain a radiation modulation block. As the basic elements of this block, mechanical choppers of radiation are usually used. They provide the complete amplitude modulation of a radiation flux. The shortcomings of those elements are their unsatisfactory compatibility with modern digital systems of electric signal processing and the possibility of the extra noise emergence stemming from mechanical system vibrations. A high degree of compatibility with digital systems of signal processing is typical of germanium injection modulators with electronic control, which operate in the spectral range 6 to 14 μm [2]. The principle of operation of these modulators is based on the phenomenon that the absorption of IR radiation in a semiconductor crystal changes under the influence of a control voltage. However, we revealed [3] that injection modulators generate a parasitic optical signal in the measuring channel [3]. That is why there is almost nothing in the

literature concerning the specificity of their use for the modulation of low-power IR radiation fluxes.

Below, we study the features of the parasitic radiation by injection modulators and its amplitude and phase characteristics. We also propose methods to minimize the influence of this radiation for the sake of constructing the devices to measure weak fluxes of IR radiation. The coefficient of IR absorption k for semiconductors in the long-wave range beyond the intrinsic absorption edge is determined by the electron, n , and hole, p , concentrations as $k = \sigma_n n + \sigma_p p$, where σ_n and σ_p are the absorption cross-sections of electrons and holes, respectively. The magnitudes of σ_n and σ_p , depending on the material and the radiation wavelength, substantially differ from one another for the majority of semiconductors.

Let us consider a modulator with thickness d (Fig. 1) fabricated of n -germanium ($n > p$). In this case, we may assume that $k = \sigma_n n$. The radiation flux T transmitted through the modulator is connected with the flux incident onto it by the relation

$$T = T_0 \frac{(1 - R)^2 e^{-kd}}{1 - R^2 e^{-2kd}}, \quad (1)$$

where R is the reflection coefficient. Usually, the quantities k and d are selected small to provide a high initial transmittance of the modulator. Accordingly, expression (1) makes allowance for the repeated reflections of radiation in the crystal. If there is a $p - n$ junction in the crystal, and a current runs through it (a forward bias is applied), the minority charge carriers (holes, in this case) are injected into the semiconductor. In germanium, the absorption cross-section for holes σ_p is larger than that for electrons σ_n . Moreover, the concentration of introduced (nonequilibrium) holes can be much higher than the concentration of equilibrium electrons. Therefore, if holes are injected, the radiation flux T_i generated by the modulator can be strongly

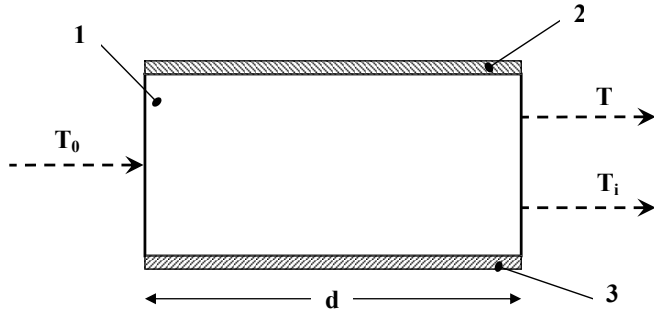


Fig. 1. Injection modulator: germanium (1), injection (2) and ohmic (3) contacts

reduced in comparison with T :

$$T_i = T_0 \frac{(1-R)^2 e^{-(k+\Delta k)d}}{1-R^2 e^{-2(k+\Delta k)d}}, \quad (2)$$

where Δk is the increment of the absorption coefficient stimulated by nonequilibrium holes.

The modulator operation is usually characterized by a parameter referred to as the modulation depth m :

$$m = \frac{T - T_i}{T} = 1 - \frac{(1-R^2 e^{-2kd}) e^{-\Delta kd}}{1-R^2 e^{-2(k+\Delta k)d}}. \quad (3)$$

As is evident from expression (3), the modulation depth m tends to its maximum (unity), if d infinitely increases. However, obtaining large modulation depths through increasing the modulator thickness is accompanied by a reduction of the initial transmittance of T . In practice, such a modulator is not always satisfactory, though its parameter m can be large.

Therefore, while analyzing the modulator operation, such a parameter as the modulation efficiency η is also used:

$$\eta = \frac{T - T_i}{T_0} = \frac{(1-R)^2 e^{-kd}}{1-R^2 e^{-2kd}} - \frac{(1-R)^2 e^{-(k+\Delta k)d}}{1-R^2 e^{-2(k+\Delta k)d}}. \quad (4)$$

This parameter enables the incident and modulated radiation fluxes to be compared. Formula (4) demonstrates that, in the ideal case, the transmitted flux T is equal to T_0 , and the flux T_i is zero if holes are injected (it is an analog of a mechanical modulator). In this case, the modulation efficiency is maximal ($\eta = 1$). By analyzing expression (4), we can find the R - and d -values, at which η tends to the maximum. In Fig. 2, the dependences of η on d at various R 's are depicted. The coefficients $k = 0.1 \text{ cm}^{-1}$ and $\Delta k = 10 \text{ cm}^{-1}$ were taken as such that could be realized experimentally.

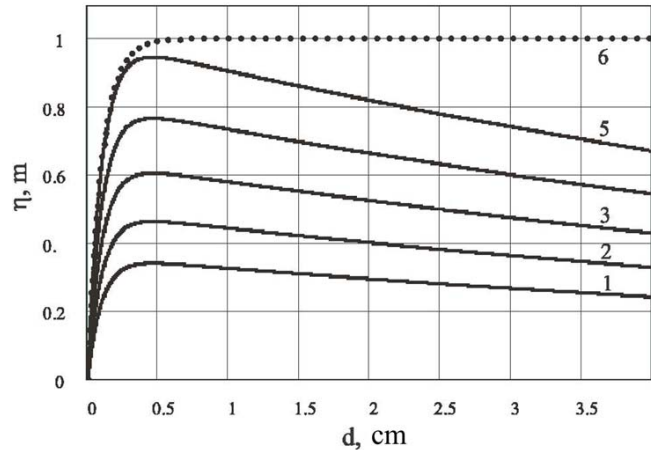


Fig. 2. Dependences of the modulation efficiency η (1 to 5) and the modulation depth m (6) on the modulator thickness d for various reflection coefficients $R = 0.4$ (1), 0.3 (2), 0.2 (3), 0.1 (4), and 0 (5)

Figure 2 demonstrates that the modulation efficiency increases as the parameter R reduces. The parameter η reaches its maximal value at $d \approx 0.4 \div 0.6 \text{ cm}$ and $R = 0$. The same figure exhibits the dependences of m on d and R . These are shown as a single curve 6, because the curves $m(d, R)$ coincide at all selected R -values (from 0.4 to 0). At $d \approx 0.6 \text{ cm}$, the modulation depth reaches its maximal possible value $m = 1$.

Hence, the injection modulator can provide not only a complete modulation ($m = 1$), but its efficiency η can also be close to unity at the corresponding values of the parameters d , R , k , and Δk . Note that in order to obtain high values of the parameter η , the working faces of modulator must be coated to reduce R .

In our experimental researches, we used an installation, the main blocks of which were a source of radiation, an injection modulator, and a radiation detector. A black body heated up to a temperature of $300 \text{ }^\circ\text{C}$ was used as a source of IR radiation. The radiation intensity was controlled with the help of calibrated diaphragms. Modulators $1.5 \times 1.5 \times 6 \text{ mm}^3$ in dimensions were fabricated of an n -Ge single crystal oriented in the (100) plane. The crystals were supplied with injection and ohmic contacts located on opposite wide faces. Radiation passed through polished mirror crystal faces $1.5 \times 1.5 \text{ mm}^2$ in dimensions with $R = 0.36$ (antireflection coatings were absent). Modulators were mounted on a copper radiator. A control voltage in the form of rectangular $21\text{-}\mu\text{s}$ pulses characterized by a pulse ratio of 2 was provided to the modulator. The voltage

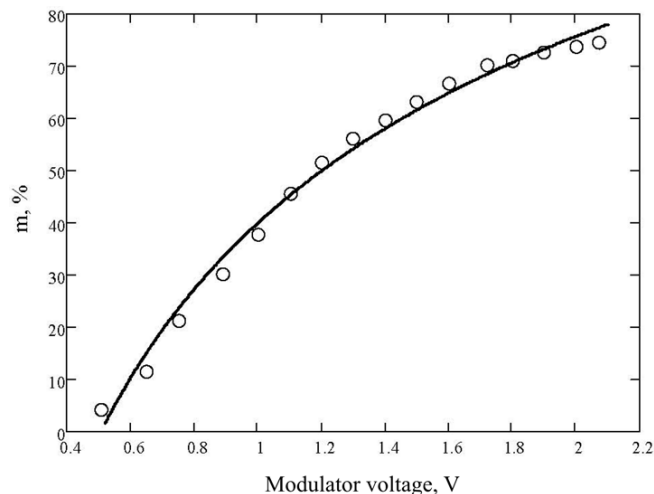


Fig. 3. Dependence of the modulation depth m on the operating voltage

amplitude was varied from 0 to 3 V (Fig. 3). A non-cooled pyroelectric detector with a LiTaO₃-based sensor was used to register radiation.

The main factor that complicates the use of an injection modulator in the optical scheme is its heating by a working current. At a voltage of about 1.3 – 1.5 V, which provides the maximal modulation depth, an increase $\Delta\theta_0$ of the average modulator temperature with respect to the ambient temperature is observed. The magnitude of $\Delta\theta_0$ is 8 – 10 °C. In addition, there appears the alternating component of a temperature increment $\Delta\theta(t)$ of a few degrees in amplitude. Hence, the modulator is a semitransparent object with a modulated temperature increment $\Delta\theta(t)$ and the modulated greyness coefficient $A(t)$, i.e. it is an object that emits its own modulated thermal radiation.

According to the aforesaid, the parasitic thermal radiation flux generated by a modulator consists of two components. One of them depends on the average temperature increment of the modulator and the alternating component of the greyness coefficient $A(t)$. The other depends on the alternating component of the modulator temperature increment $\Delta\theta(t)$ and the average value of the greyness coefficient A_0 . In this approximation, we neglect the components of higher orders, which arise due to a combined action of the variable factors $A(t)$ and $\Delta\theta(t)$.

Since the growth of the greyness coefficient of the modulator is accompanied by a reduction of its transparency, either the first component of parasitic signal coincides by phase with the useful radiation flux or they are in antiphase (depending on the relation between

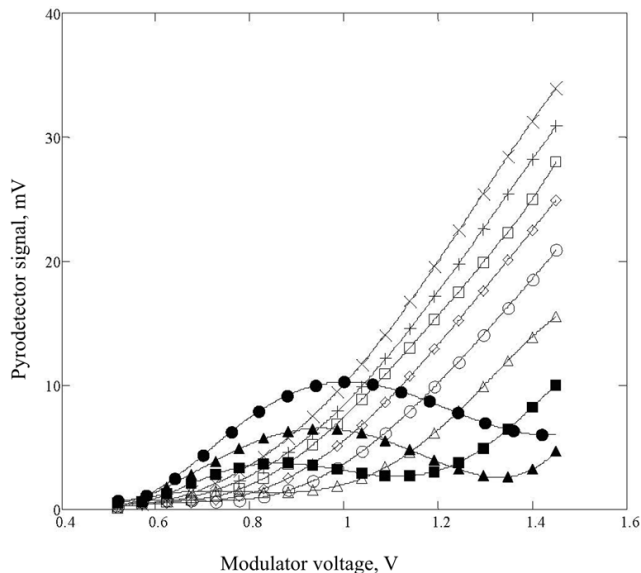


Fig. 4. Dependences of the radiation detector signal amplitude on the control modulator voltage for various diameters of the black-body output aperture: 0 (x), 3 (+), 4 (◇), 5 (□), 6 (○), 7 (△), 8 (●), 9 (▲), and 10 mm (■)

the temperatures of the modulator and the object). The analysis of thermal processes in the modulator [6] testifies that the phase shift of the second parasitic component amounts to 90 °C, provided that thermal losses are low: $G \ll \omega C$, where G is the effective heat conductivity of the modulator, C its heat capacity, and ω the modulation frequency.

In Figs. 4 and 5, the experimental dependences of the amplitude and the phase shift, respectively, of a radiation detector signal on the amplitude of modulator control voltage are depicted for various measured heat fluxes. The latter were varied with the help of a set of diaphragms possessing various diameters and installed at the output of the radiation source, the black body. The parasitic fluxes are clearly seen to substantially distort the results of measurements of weak signals. In the range of low control voltages, the phase shift approaches 90°, which evidences for a dominating role of the second component associated with the emergence of the alternating component in the modulator temperature increment.

In the range of high control voltages, we observe that the first component plays a dominant role; it depends on the average modulator temperature increment $\Delta\theta_0$ and the alternating component of the greyness coefficient $A(t)$, which, in our case, is in antiphase to the useful signal. In the range of moderate control voltages, when

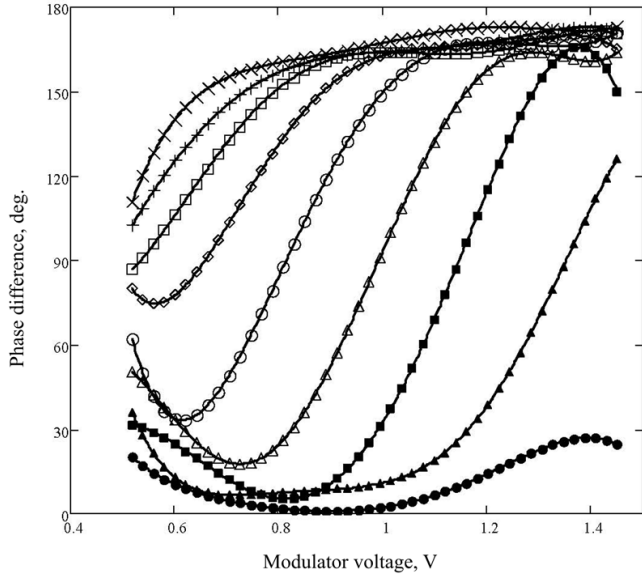


Fig. 5. Dependences of the phase shift of the radiation detector signal on the operating modulator voltage for various diameters of the black-body output aperture: 0 (×), 3 (+), 4 (◇), 5 (□), 6 (○), 7 (△), 8 (●), 9 (▲), and 10 mm (■)

the parasitic flux induced by the growth of the average modulator temperature does not exceed the useful one, the latter governs the phase of the total signal. If the control voltage increases further, the growth of the parasitic component gives rise to a reduction of the total signal down to a complete compensation of the parasitic and useful components. After that, the phase changes by 180° . This fact testifies to the dominant role of the parasitic component.

The most important is the range of high control voltages, because it corresponds to optimum values of the modulation coefficient. Therefore, an urgent problem is to compensate the average temperature increase of the modulator in its operating mode. For this purpose, we used a system of forced modulator cooling making use of a Peltier element. In this case, the modulator is supplied with a control voltage that provides a required modulation coefficient. Such an operating regime should be selected for the Peltier element that the modulator temperature would decrease and become equal to the ambient one. In Fig. 6, the dependences of the amplitude and the phase shift of a pyroelectric detector signal on the current through the Peltier element are shown in the case where the environment is a source of external optical radiation.

The increase of the current through the Peltier element from 0 to 1.5 A corresponds to the change of

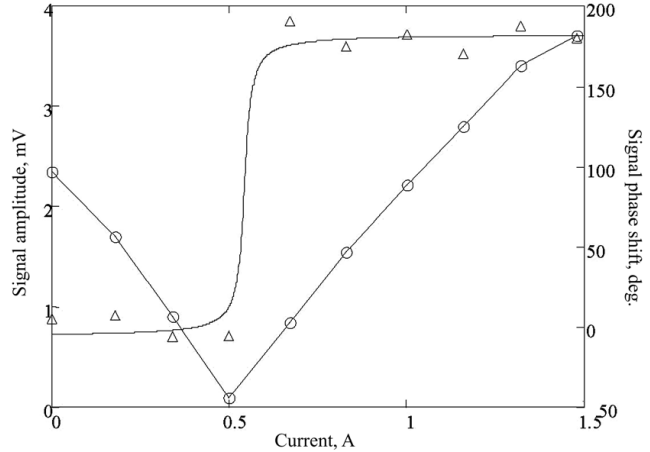


Fig. 6. Dependences of the amplitude (○) and the phase shift (△) of the parasitic signal of a pyroelectric detector on the current through a Peltier element

the temperature difference between the modulator and the environment from $+7$ to -11 °C. At a current of 0.5 A through the Peltier element, both $\Delta\theta$ and the output signal of the detector tend to zero. Note that, if the modulator temperature is elevated (the current through the Peltier element equals 0–0.5 A), the intensity of the parasitic modulator radiation grows together with the growth of the control voltage applied to the modulator. On the contrary, in the interval 0.5–1.5 A, the intensity diminishes. This fact is testified by a change of the phase difference between the reference and pyrodetector signals (Fig. 6). Temperature compensation allows us to control only the in-phase component of a parasitic signal. Therefore, it is impossible to eliminate the parasitic signal completely. At point, where it is minimal, there always remains a certain “pedestal” depending on the quadrature component which is connected, in turn, with the alternating component of the modulator temperature increment.

For the compensation of parasitic components to be complete, we proposed a two-channel compensatory scheme [3–5]. Two identical modulators are mounted side-by-side on a radiator (without a Peltier element). The useful optical signal passes through one of them. Radiation generated by the blackened object, which is the tiny model of a black body with ambient temperature, falls onto the other. Radiation from both modulators is directed to the detector through a reduction system. In this design, the identical parasitic fluxes from both modulators operating in antiphase are subtracted, which provides an adequate stable

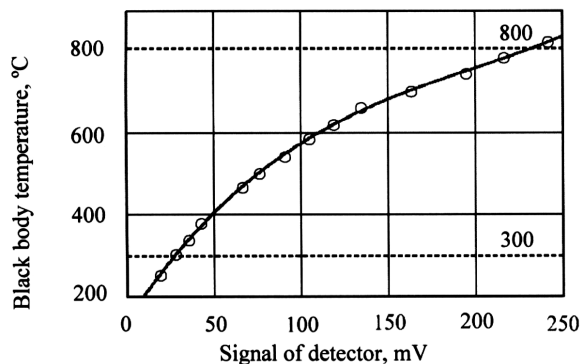


Fig. 7. Calibration curve of the device in the temperature range 200 – 800 °C

of the injection modulator block. Optical matching between a section of the heated solid and the pyroelectric radiation detector is provided with the use of an optical system for introducing the radiation, which is fulfilled according to a mirror-lens design of the Cassegrain type with a sighting device operating in the visible spectral range.

The detector was made of a pyroelectric LiTaO_3 crystal. It was placed in a microcircuit case with a germanium input window. To maximize the device sensitivity for measuring the temperatures close to the lower limit of its dynamic range, the input window was covered with a broadband antireflecting coating characterized by a transmittance maximum at the wavelength $\lambda \approx 9 \mu\text{m}$. A thin absorbing coating (the absorption coefficient was not lower than 95%) was deposited onto the frontal surface of the sensor. This construction provided a high uniform spectral sensitivity within the whole IR spectral range. The sensitive area diameter was 2 mm; the detector sensitivity was 10^3 V/W ; the supply voltage was $\pm 15 \text{ V}$, the output resistance was not higher than $1 \text{ k}\Omega$, and the threshold sensitivity was $5 \times 10^{-10} \text{ W/Hz}^{1/2}$.

In a close vicinity to the pyroelectric radiation detector, we placed an ambient temperature sensor (a thermodiode), which allowed temperature fluctuations

to be taken into account and a calibration plot—common for all ambient temperatures—to be used (Fig. 7).

On the basis of the developed module “modulator–pyrodetector”, a series of noncontact sensors for measuring the local temperatures in the range 200–2000 °C have been created. The sensors can be used in automatic control systems for technological processes (laser and electron-beam welding, zone melting), as well as for the diagnostics of objects that are located in hard-to-reach areas (furnaces, engines, high-voltage equipment, and so on).

1. V.F. Kosorotov, L.S. Kremenchugskii, V.B. Samoylov, and L.V. Shchedrina, *Pyroelectric Effect and Its Practical Applications* (Naukova Dumka, Kyiv, 1989) (in Russian).
2. E.R. Mustel' and V.N. Parygin, *Methods of Light Modulation and Scanning* (Nauka, Moscow, 1970) (in Russian).
3. M.Yu. Vedula, L.V. Levash, A.I. Liptuga *et al.*, *Heat Transf. Res.* **36**, 21 (2005).
4. L.V. Levash, A.I. Liptuga, and V.B. Samoylov, *Ukrainian patent certificate No. 34740* of 15.06.2001 (in Ukrainian)
5. L.V. Levash, A.I. Liptuga, and V.B. Samoylov, *Russian patent certificate No. 2159414* of 20.11.2000 (in Russian)
6. H.S. Carslaw and J.C. Jaeger, *Conduction of Heat in Solids* (Oxford Univ. Press, London, 1959).

Translated from Ukrainian by O.I. Voitenko

БЕЗКОНТАКТНІ ПІРОЕЛЕКТРИЧНІ ВИМІРЮВАЧІ ТЕМПЕРАТУРИ З ТВЕРДОТІЛЬНИМ МОДУЛЯТОРОМ

*Л.В. Леваши, А.І. Ліптуга, В.С. Лисенко,
Ю.Г. Птушинський, В.Б. Самойлов*

Резюме

Досліджено властивості інжекційного напівпровідникового модулятора інфрачервоного (ІЧ) випромінювання і встановлено, що він є джерелом власного теплового випромінювання, яке суттєво ускладнює вимірювання слабких радіаційних потоків. Досліджено особливості цього випромінювання та розроблено оригінальний модулюючий блок, що дозволяє компенсувати вплив випромінювання модулятора на точність вимірювання потоків малої потужності. Описано конструкцію, принципи дії та основні параметри піроелектричного безконтактного вимірювача температури з електронною модуляцією випромінювання.